Molecular Therapy
Nucleic Acids
Original Article

Codon-dependent translation of N1-ethylpseudouridine-modified mRNA reduces innate immunity while preserving vaccine immunogenicity

Jisang Park,[1,6] GeonHee Lee,[2,4,6] Haneul Lee,[1,3,6] Ju Kim,[1] Kyeongmi Kim,[2] Eunsook Kim,[2,5] Jiyoung Lee,[2,5] Sangwook Lee,[2] Jeehee Youn,[4] and Yong-Suk Jang[1,3]

[1]Department of Molecular Biology and the Institute for Molecular Biology and Genetics, Jeonbuk National University, Jeonju 54896, Korea; [2]mCureX Therapeutics, Seoul 05854, Korea; [3]Department of Bioactive Material Sciences and Research Center of Bioactive Materials, Jeonbuk National University, Jeonju 54896, Korea; [4]Department of Anatomy and Cell Biology, College of Medicine, Hanyang University, Seoul 04763, Korea

Messenger RNA (mRNA) vaccines are a versatile platform for rapid vaccine development; however, nucleoside modifications must be optimized to balance translational efficiency and innate immune activation. Here, we evaluated N1-ethylpseudouridine (Et1Ψ) as an alternative to the widely used N1-methylpseudouridine (m1Ψ). Et1Ψ-modified mRNA exhibited a distinct codon-dependent translational sensitivity, with increased UUU codon content leading to reduced protein expression. Importantly, synonymous codon optimization that eliminated UUU codons restored translation efficiency to levels comparable to those of m1Ψ-modified mRNA across multiple cell types. Despite this constraint, Et1Ψ consistently reduced innate immune activation *in vitro* and *in vivo*. Following codon optimization, Et1Ψ-modified mRNA supported robust protein expression comparable to that from m1Ψ-modified mRNA. When applied to vaccine antigens, including SARS-CoV-2 spike and tetravalent dengue envelope domain III constructs, Et1Ψ-modified mRNA elicited strong humoral and cellular immune responses, with neutralizing activity comparable to that of m1Ψ-modified mRNA. Collectively, these findings identify Et1Ψ as an alternative nucleoside modification that combines reduced innate immunogenicity with codon-aware sequence optimization, highlighting codon-modification interactions as a key design principle for mRNA therapeutics.

INTRODUCTION

The concept of using messenger RNA (mRNA) as a therapeutic platform was first introduced in the late 1980s, following the demonstration that *in vitro*-transcribed mRNA could produce proteins in mammalian cells. However, early applications of mRNA were limited by the molecule's inherent instability, rapid degradation by extracellular RNases, and strong innate immune activation.[1] During the 1990s and early 2000s, advances in mRNA engineering, including improved capping, polyadenylation, and delivery technologies, gradually enhanced mRNA stability and translational efficiency, establishing the foundation for practical therapeutic applications.[2] Building on these developments, mRNA vaccines have emerged as a new immunization technology that uses synthetic mRNA to encode specific antigens to induce protective immunity. Once delivered into host cells, the mRNA is translated into target proteins that mimic those expressed by infectious agents or malignant cells, which are subsequently recognized by the immune system and trigger humoral and cellular immune responses.[3] To protect the RNA from degradation and promote efficient cellular uptake, mRNA is usually encapsulated in lipid nanoparticles (LNPs), which facilitate its delivery into the cytoplasm.[4] In contrast to conventional vaccine platforms, mRNA vaccines offer several benefits, including rapid design, scalable production, relatively low cost, and the ability to induce strong adaptive immune responses without integrating into the host genome.[5] The COVID-19 pandemic, caused by SARS-CoV-2, dramatically accelerated the development and approval of this technology, leading to rapid authorization and worldwide distribution of mRNA vaccines such as BNT162b2 and mRNA-1273, which demonstrated impressive effectiveness and safety in large clinical trials.[6,7] This success was achieved through key technological advances, including improved mRNA stabilization techniques, nucleoside modifications such as N1-methylpseudouridine (m1Ψ), and optimized LNP delivery systems.[8] Together, these developments not only facilitated an effective response to the pandemic but also

Received 8 April 2026; accepted 1 September 2026;
https://doi.org/10.1016/j.omtn.2026.103082.

[5]Present address: R&D Institute, Daehan Nupharm Co., Ltd., Seongnam 13449, Korea

[6]These authors contributed equally

Correspondence: Jeehee Youn, Department of Anatomy and Cell Biology, College of Medicine, Hanyang University, Seoul 04763, Korea.
E-mail: jhyoun@hanyang.ac.kr
Correspondence: Yong-Suk Jang, Department of Molecular Biology and the Institute for Molecular Biology and Genetics, Jeonbuk National University, Jeonju 54896, Korea.
E-mail: yongsuk@jbnu.ac.kr

Published by Elsevier Inc. on behalf of The American Society of Gene and Cell Therapy.
This is an open access article under the CC BY-NC-ND license (http://creativecommons.org/licenses/by-nc-nd/4.0/).

positioned mRNA as a flexible platform for quickly developing vaccines against new infectious diseases.[9]

Pseudouridine (Ψ), the most common naturally occurring RNA modification, accounts for approximately 9% of uridine residues in total RNA and is present in tRNA, rRNA, mRNA, and small nuclear RNAs, where it enhances RNA structural stability and protein interactions.[10] Structurally, Ψ is an isomer of uridine where the β-D-ribose is linked to the C5 position of the uracil ring, conferring unique biophysical properties such as enhanced base stacking and hydrogen-bonding potential.[10] Incorporating Ψ into synthetic RNA decreases immunogenicity by impairing lysosomal processing, thereby preventing the RNase T2-and phospholipase D-mediated formation of TLR7-and TLR8-activating fragments. Meanwhile, m1Ψ can still activate TLR8 if released from the RNA backbone.[11] In mRNA vaccination, dendritic cells and macrophages in draining lymph nodes take up the modified RNA and produce the encoded spike proteins, which trigger a strong innate immune activation and cytokine production, including IL-6, IFN-α, IFN-γ, MCP-1, and MIP-1β. This response is critically dependent on the MDA5-IFNAR1 signaling pathway, which is also essential for activating $CD8^+$ T cell responses in the spleen and lung tissues.[12]

To investigate whether increased N1 steric bulk could reduce innate immune sensing without compromising mRNA performance, we evaluated N1-ethylpseudouridine (Et1Ψ) as an alternative to m1Ψ.[13] We hypothesized that Et1Ψ might attenuate innate immune activation, while its larger N1 substituent could impose sequence-dependent constraints on translation. We therefore compared Et1Ψ with m1Ψ in reporter and vaccine-antigen mRNAs and tested whether targeted synonymous recoding could preserve protein expression. Et1Ψ reduced innate signaling relative to m1Ψ in several settings, whereas its UUU-dependent translational limitation was mitigated by replacing UUU with UUC. Across SARS-CoV-2 spike and tetravalent dengue EDIII (tetEDIII) constructs, codon-adjusted Et1Ψ mRNA maintained adaptive immune responses comparable to those of m1Ψ mRNA. These findings define a potential advantage and a specific sequence design requirement for Et1Ψ-based mRNA platforms.

RESULTS

Codon optimization rescues UUU-dependent translational suppression of Et1Ψ-modified mRNA

Previous studies demonstrated that codon identity and synonymous codon usage can significantly influence translational efficiency and protein production, with some synonymous codons (e.g., the UUU codon for phenylalanine) showing context-dependent effects on translation speed and yield due to differences in decoding kinetics and tRNA engagement.[14,15] Moreover, chemical modification of mRNA bases, such as N1-methylpseudouridine (m1Ψ), modulates ribosome-decoding dynamics in a sequence-dependent manner, suggesting that the combined impact of codon context and base modification can affect translation outcomes.[16] Building on these findings, we investigated whether UUU codon frequency interacts with uridine modification to influence translational efficiency. We generated luciferase-encoding mRNAs containing increasing numbers of UUU codons in the open reading frame and modified them with either m1Ψ or Et1Ψ (Figure 1A). In HEK293 cells, m1Ψ-modified mRNA displayed stable luciferase expression regardless of UUU-codon content (Figure 1B). By contrast, Et1Ψ-modified mRNA exhibited a pronounced, UUU-dependent reduction in luciferase activity, with constructs having higher UUU frequencies showing progressively diminished translation. Notably, replacing UUU codons with synonyms significantly restored luciferase expression from Et1Ψ-modified mRNA, yielding translation levels similar to those of m1Ψ-modified mRNA (Figure 1B). A similar pattern was observed in HeLa cells, a distinct epithelial cell line with different translational and metabolic characteristics (Figure 1C). As in HEK293 cells, m1Ψ-modified mRNA remained largely insensitive to UUU codon frequency, whereas Et1Ψ-modified mRNA showed marked translational suppression as UUU content increased. Once again, removing UUU codons effectively rescued luciferase expression, indicating that the UUU-related translational impairment of Et1Ψ-modified mRNA is consistent across different cell types (Figure 1C). Together, these results demonstrate that Et1Ψ-mediated translational suppression is influenced by sequence context rather than cell type-specific factors, and that codon optimization enables robust protein expression from Et1Ψ-modified mRNA across different cellular environments.

Et1Ψ-mediated mRNA facilitates efficient protein expression with reduced innate immune signaling *in vitro*

In contrast to unmodified uridine, m1Ψ decreases innate immune activation while still enabling efficient protein production, laying the groundwork for its widespread adoption in current mRNA platforms.[17] We first examined whether Et1Ψ similarly lessens innate immune signaling *in vitro*. We transfected THP-1 reporter cells with mRNA containing uridine, m1Ψ, or Et1Ψ modification. Protein expression was quantified independent of the innate immune response, enabling a direct comparison of translation efficiency and immune activation (Figure 2A). Et1Ψ-modified mRNA achieved protein levels comparable to those achieved by m1Ψ-modified mRNA, with no significant difference between them. However, the interferon regulatory factor (IRF)-dependent reporter activity in Et1Ψ-modified mRNA was significantly lower than in unmodified uridine and lower than that in m1Ψ-modified mRNA (Figure 2A).

Et1Ψ-modified mRNA maintains robust *in vivo* expression with minimal systemic interferon induction

We then assessed protein expression from Et1Ψ-modified mRNA *in vivo*. Longitudinal *in vivo* bioluminescence imaging (IVIS) scans showed different expression patterns depending on the mRNA modification (Figure 2B). At 6 h after injection, m1Ψ- and Et1Ψ-modified mRNAs produced strong bioluminescent signals, with the levels of Et1Ψ-driven expression comparable to those of m1Ψ-driven expression and markedly higher than those of unmodified uridine-driven expression. By 24 h, bioluminescence from m1Ψ- and Et1Ψ-modified mRNAs remained high and not

significantly different. At 72 h, the signals decreased in all groups. At 168 h, the bioluminescent signals from all groups declined to near-baseline levels, with no notable differences among the modification conditions. The serum levels of type I and II interferons were measured 6 h post-injection to evaluate innate immune activation *in vivo* (Figure 2C). Unmodified uridine mRNA induced measurable increases in IFN-α and IFN-γ, whereas m1Ψ-modified mRNA elicited lower cytokine levels. Compared with unmodified uridine, Et1Ψ-modified mRNA decreased IFN-α levels to near baseline. Conversely, IFN-γ levels induced by Et1Ψ-modified mRNA were significantly lower than those induced by unmodified uridine (Figure 2C). Poly(I:C) administration strongly increased the levels of both cytokines, confirming innate immune activation. These findings indicate that Et1Ψ-modified mRNA achieves protein expression comparable to that achieved by m1Ψ-modified mRNA while eliciting minimal systemic interferon responses.

Codon-dependent translation of Et1Ψ-modified mRNA is preserved in vaccine antigens

To assess whether the UUU-dependent translation behavior observed in reporter mRNAs also applies to vaccine-relevant antigens, we incorporated Et1Ψ into two antigen constructs: SARS-CoV-2 spike (S) and a tetEDIII antigen. Initially, we determined whether the previously noted reduction in translation in UUU-rich contexts also occurs in these antigens and whether removing UUU codons can restore expression. HeLa cells were transfected with spike mRNA containing either 15 UUU codons (UUU = 15) or a UUU-depleted variant (UUU = 0), synthesized with unmodified uridine, m1Ψ, or Et1Ψ. When UUU = 15, Et1Ψ-modified spike mRNA showed lower protein expression than U- and m1Ψ-modified mRNAs. Conversely, under UUU = 0 conditions, spike expression from Et1Ψ-modified mRNA was restored to levels comparable to that from U- and m1Ψ-modified mRNAs (Figure 3A), indicating that the translation issue depends on UUU codon content rather than the antigen type. We tested tetEDIII with UUU depletion. HeLa cells transfected with U-, m1Ψ-, or Et1Ψ-modified tetEDIII mRNA exhibited similar protein expression across all modifications (Figure 3B), further confirming that UUU codon removal restores Et1Ψ-driven translation across distinct antigen constructs.

Et1Ψ-modified antigen mRNA reduces systemic inflammatory responses *in vivo*

Whether Et1Ψ retains its reduced innate immune activation profile in an antigen context was determined by injecting BALB/c mice intravenously with spike mRNA and measuring serum cytokines after 6 h (Figure 3C). Et1Ψ-modified mRNA caused significantly lower levels of IFN-α and IFN-γ than unmodified uridine and m1Ψ-modified mRNAs (Figure 3C), indicating attenuation of early systemic interferon responses. In contrast to unmodified uridine mRNA, which elicited marked increases in inflammatory cytokines approaching levels observed in poly(I:C)-treated mice, Et1Ψ-modified mRNA was associated with significantly reduced induction of multiple inflammatory mediators, including IL-6, MIP-1α, MIP-1β, CXCL10, and MCP-1. Compared with m1Ψ-modified mRNA, Et1Ψ-modified mRNA induced significantly lower levels of CXCL10 and MCP-1, supporting a diminished inflammatory profile *in vivo*. Collectively, these results indicate that Et1Ψ-modified mRNA supports efficient antigen expression after UUU codon removal and results in lower systemic interferon and inflammatory cytokine responses *in vivo* than unmodified uridine while maintaining expression levels comparable to m1Ψ-modified mRNA.

Et1Ψ-modified mRNA induces robust humoral and cellular immune responses against SARS-CoV-2

Et1Ψ-modified mRNA-LNP was evaluated to determine whether its reduced innate immune activation profile affects adaptive immune responses when used as a vaccine against SARS-CoV-2. BALB/c mice were immunized using a prime-boost regimen (5 μg) of spike-encoding mRNA-LNPs (Figure 4A). ELISA on day 35 revealed that Et1Ψ induced high titers of S1- and RBD-specific IgG antibodies, with levels comparable to those elicited by m1Ψ-modified mRNA-LNPs (Figure 4B). For full-length spike (S), the IgG titers in the m1Ψ group increased by approximately 8–10-fold compared with those in the mock group, whereas Et1Ψ elicited a comparable magnitude of increase. Similarly, RBD-specific IgG levels were elevated by roughly an order of magnitude over mock controls in m1Ψ- and Et1Ψ-immunized mice. Statistical analysis confirmed that both modified mRNA groups showed significant increases compared with the mock group, whereas no statistically significant difference was observed between the m1Ψ and Et1Ψ groups for either S- or RBD-specific IgG responses. These data indicate that Et1Ψ elicits antibody responses comparable in quantity to the established m1Ψ platform. IFN-γ ELISPOT (enzyme-linked immunospot) analysis revealed a marked increase in spike-specific T cell responses in both m1Ψ- and Et1Ψ-immunized mice compared with mock controls (Figure 4C). Upon peptide stimulation, the frequency of IFN-γ-secreting cells increased by approximately 8–10-fold relative to mock levels, with no significant difference between the m1Ψ and Et1Ψ groups. IL-4 ELISPOT responses were also elevated after vaccination (Figure 4C); however, the magnitude of IL-4-secreting cells was substantially lower than that of IFN-γ-secreting cells, indicating a predominantly Th1-skewed cellular immune response. Although the m1Ψ and Et1Ψ groups showed significant increases compared with the mock control, no significant difference was observed between the two modification platforms.

Et1Ψ-modified mRNA induces neutralizing antibody responses against SARS-CoV-2

Neutralizing activity was assessed against the ancestral Wuhan strain and the Omicron variant using a pseudovirus neutralization assay (Figure 4D). Mice immunized with spike mRNA-LNPs exhibited robust neutralizing responses against the Wuhan strain compared with the mock control. The 5 μg dose group showed a further increase, indicating a dose-dependent boost in neutralizing activity. Statistical analysis confirmed that the neutralization titers in the 5 μg group were significantly higher than those in the mock and 1 μg groups. When tested against the Omicron variant, the neutralization titers were lower than those against the Wuhan strain,

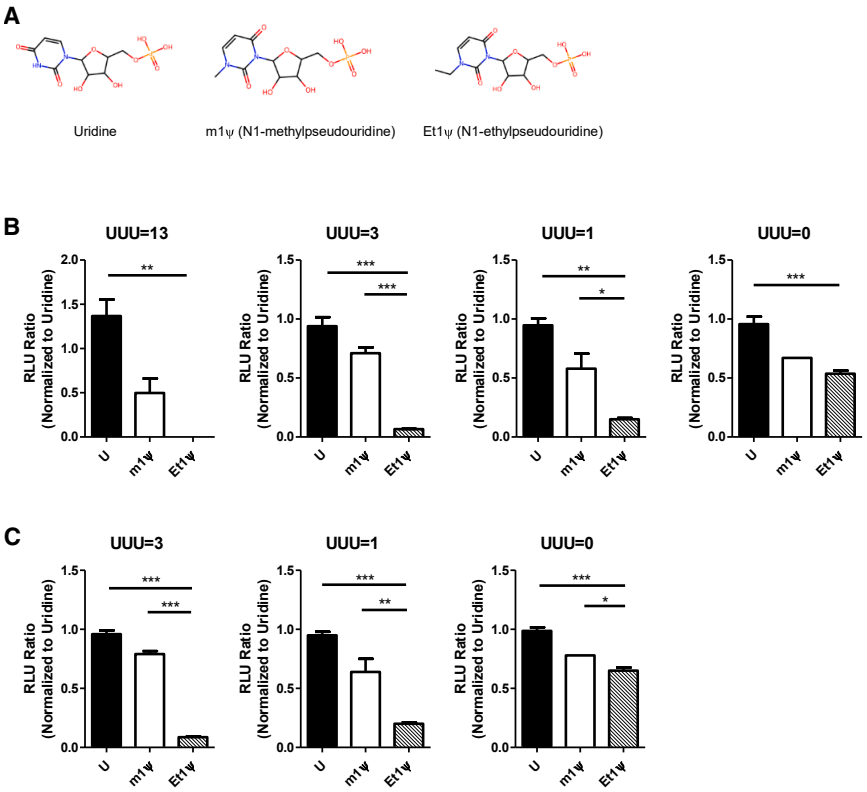


Figure 1. Structures and UUU-dependent translation of uridine variants

(A) Chemical structures of uridine, N1-methylpseudouridine (m1Ψ), and N1-ethylpseudouridine (Et1Ψ). (B and C) Luciferase expression from mRNAs containing the indicated numbers of UUU codons (UUU = 13, 3, 1, or 0) in HEK293 (B) and HeLa (C) cells. Cells were transfected with 0.25 μg/mL FLuc mRNA, and luciferase activity was measured 24 h post-transfection. Data are presented as mean ± SD from three independent biological experiments ($n = 3$); each experiment was performed in technical triplicate. Statistical significance was assessed by one-way ANOVA with Tukey's multiple-comparison test; $^{*}p < 0.05$, $^{**}p < 0.01$, $^{***}p < 0.001$.

reflecting the antigenic differences of this variant. However, both immunized groups maintained detectable neutralizing activity above mock levels. Although the increase was not statistically significant compared with the mock group, the 5 μg dose group had a higher average neutralization titer than the 1 μg group, suggesting partial cross-neutralization against Omicron. Overall, these results showed that the spike mRNA-LNP vaccination induced strong neutralizing antibody responses against the ancestral SARS-CoV-2 strain and retained some measurable, though reduced, activity against Omicron.

Et1Ψ-modified dengue mRNA vaccine induces robust humoral and cellular immune responses

Dengue virus vaccine development has been challenged by the requirement to elicit a balanced and protective immune response against four antigenically distinct serotypes while avoiding the induction of sub-neutralizing antibodies associated with antibody-dependent enhancement (ADE). Conventional vaccine platforms, including live-attenuated and protein subunit vaccines, have inherent limitations in achieving efficacy and safety, partly because of restricted control over antigen presentation and immune activation. mRNA vaccine platforms offer a promising alternative by enabling the precise control of antigen expression and promoting robust immune responses without viral replication. In this context, we applied Et1Ψ-modified mRNA to a dengue vaccine construct to enhance the expression of a tetEDIII antigen and efficiently induce immune responses, as described in the following experiments. Based on our previous experiments, we confirmed that tetEDIII expression driven by m1Ψ- and Et1Ψ-modified mRNAs showed no significant difference *in vitro* (Figure 3B). To evaluate whether these modifications differentially affect the immune response *in vivo*, we formulated each mRNA into Moderna-based LNPs and administered it via intramuscular injection three times at 15-day intervals. Serum and splenocytes were collected to assess humoral and cellular immune responses (Figure 5A). EDIII-specific serum IgG titers against each DENV serotype were measured and expressed as log2 titration values. For m1Ψ- and Et1Ψ-formulated vaccines, the mean titers were 10 and 11 for DENV1, 8.2 and 8.8 for DENV2, 9.3 and 9.9 for DENV3, and 9.4 and 10.3 for DENV4, respectively. No significant differences were observed between the two groups for any serotype (Figure 5B). At 7 days after the final immunization, the spleens were harvested, and splenocytes were isolated. Cells were stimulated with PMA (phorbol 12-myristate 13-acetate)/ionomycin or an EDIII antigen mix, and cytokine levels were quantified using a cytometric bead array kit. Although no significant differences were observed between the m1Ψ and Et1Ψ groups upon either stimulation, EDIII mix stimulation induced a robust increase in IFN-γ production in both vaccinated groups compared with the mock control (Figure 5C). By contrast, no type 2 cytokines, including IL-4, were detected. These results indicate that Et1Ψ-modified tetEDIII mRNA-LNPs induce strong humoral immunity and a predominantly Th1-biased cellular immune response.

Et1Ψ-modified dengue mRNA vaccine elicits neutralizing antibodies and confers protective immunity

We then evaluated the functional activity of the vaccine-induced antibodies. The neutralization of each DENV serotype was tested *in vitro*. Focus-reduction neutralization test 50 (FRNT50) values after the first and second boosts were 2388 and 1879 for DENV1, 97.6 and 261 for DENV2, 271 and 323 for DENV3, and 135 and 535 for DENV4, respectively. Compared with the first boost, the second boost produced a more balanced neutralizing antibody response

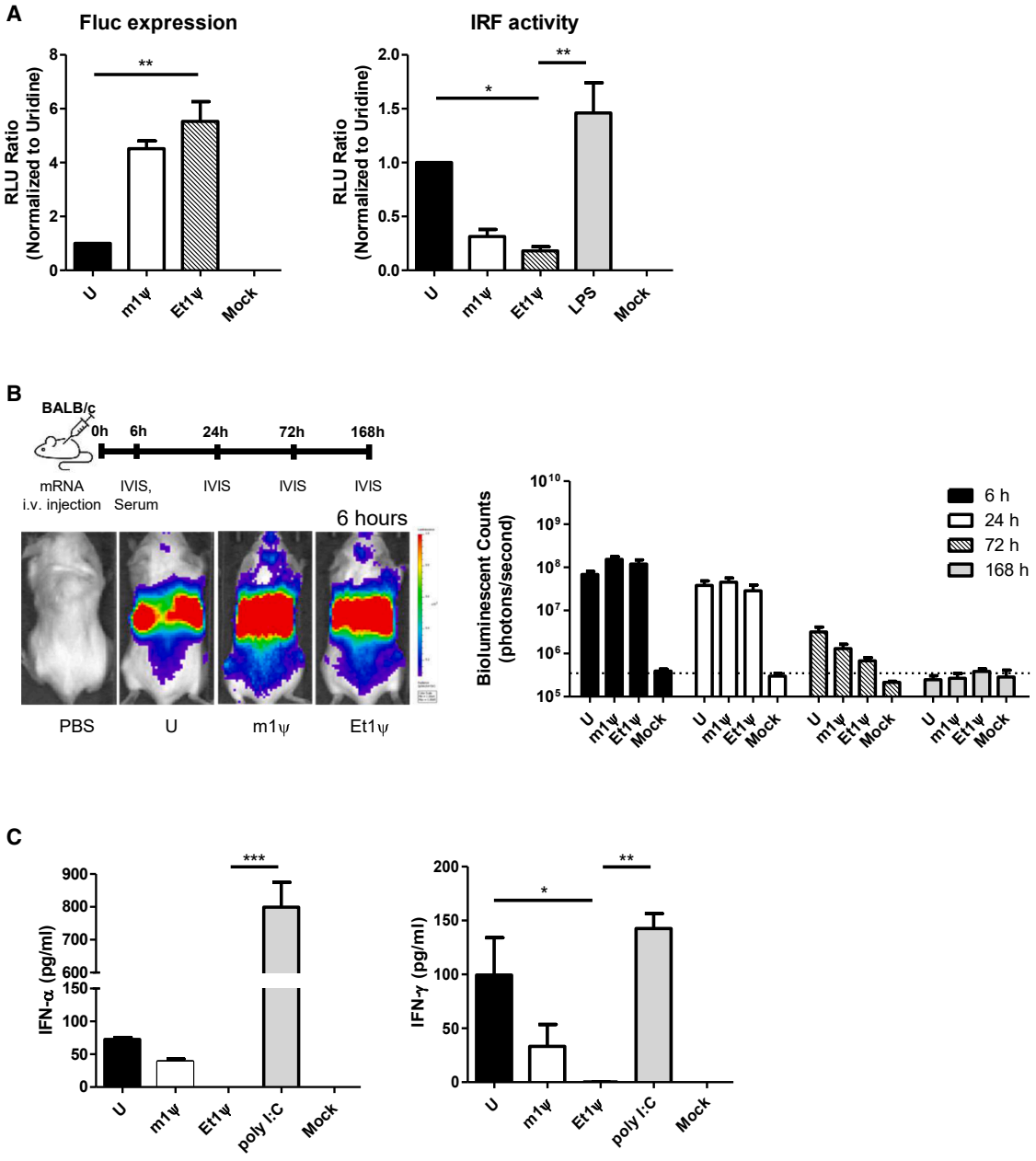


Figure 2. Protein expression and innate immune activation by modified mRNAs

(A) FLuc expression (left) and interferon regulatory factor (IRF) reporter activity (right) in activated THP-1 reporter cells transfected with 2 μg/mL MessengerMAX-formulated FLuc mRNA. Lipopolysaccharide (LPS; 0.1 μg/mL) served as the positive control for IRF activation. Data are mean ± SD from three independent biological experiments ($n = 3$). (B) *In vivo* bioluminescence after intravenous administration of TransIT-formulated FLuc mRNA (10 μg) to BALB/c mice ($n = 3$ mice per group). Representative IVIS images at 6 h (left) and total flux over 168 h (right) are shown. (C) Serum IFN-α (left) and IFN-γ (right) measured 6 h after injection in BALB/c mice ($n = 4$ mice per group). Poly(I:C) served as the positive control. Data are presented as mean ± SEM. Statistical significance was assessed by one-way ANOVA with Tukey's multiple-comparison test; $^{*}p < 0.05$, $^{**}p < 0.01$, $^{***}p < 0.001$.

across all four serotypes. To further assess protective efficacy *in vivo*, immune serum samples from vaccinated mice were passively transferred into AG129 mice before viral challenge (Figure 5E). Mice receiving sera from the Et1Ψ-vaccinated group after the second boost showed 40% survival following DENV1, DENV2, and DENV4 challenge, whereas all mock-treated mice succumbed to infection under these conditions. In the DENV3 challenge model, 100% survival was observed in the vaccinated serum group, whereas

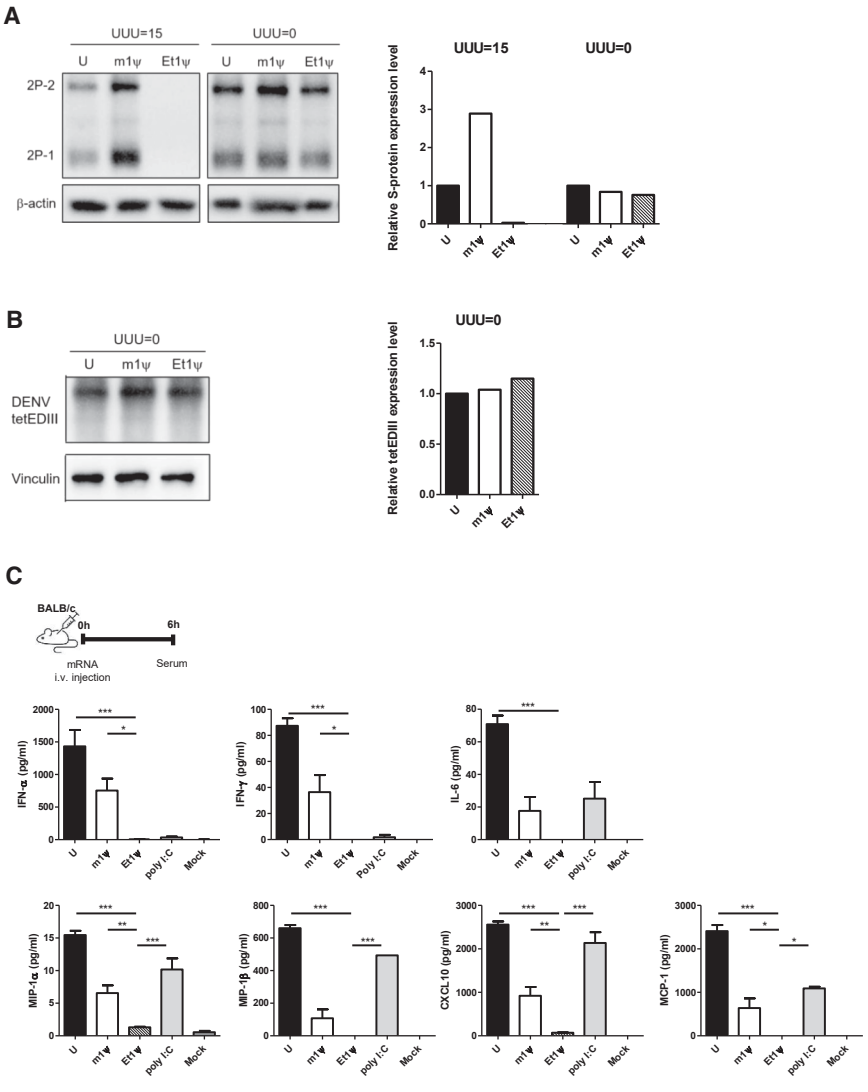


Figure 3. Antigen expression and systemic cytokine responses after UUU depletion

(A) SARS-CoV-2 spike protein expression in HeLa cells transfected with mRNA containing either the original sequence (UUU = 15) or the UUU-depleted sequence (UUU = 0). β-Actin served as the loading control. (B) DENV tetEDIII expression from the UUU-depleted construct (UUU = 0) in HeLa cells. Vinculin served as the loading control. Representative blots and densitometric quantification from two independent experiments (n = 2) are shown; each experiment was performed in technical duplicate. (C) BALB/c mice received the indicated SARS-CoV-2 spike mRNA-LNP formulations intravenously (10 μg; n = 4 mice per group), and serum was collected 6 h later. MIP-1α, CXCL10, MIP-1β, MCP-1, IL-6, IFN-α, and IFN-γ were quantified by multiplex analysis. Poly(I:C) and mock treatment served as positive and negative controls, respectively. Data are presented as mean ± SD. Statistical significance was determined by one-way ANOVA followed by Tukey's multiple-comparison test; $^{*}p < 0.05$, $^{**}p < 0.01$, $^{***}p < 0.001$.

the mock group showed 80% survival, indicating limited mortality in this setting. Overall, these findings demonstrate that Et1Ψ-modified tetEDIII mRNA vaccines induce neutralizing antibodies capable of providing serotype-dependent protection *in vivo*.

DISCUSSION

Chemical modification of uridine has been central to the development of mRNA platforms, reducing excessive innate immune sensing while maintaining translation.[6,18] In this study, Et1Ψ exhibited a clear UUU-dependent translational constraint: increasing UUU content reduced protein output, whereas targeted UUU-to-UUC replacement restored expression across reporter mRNAs and two vaccine antigens. The principal advantage of Et1Ψ was therefore conditional. Once the UUU constraint was addressed, Et1Ψ maintained protein expression and vaccine immunogenicity comparable to m1Ψ while producing lower early innate immune responses in several tested settings. Accordingly, our findings support Et1Ψ as an alternative, codon-dependent design option rather than a universally superior replacement for m1Ψ.

However, the molecular basis for the selective sensitivity of UUU remains unclear. A UUU codon places Et1Ψ at all three codon positions, whereas UUC retains Et1Ψ at the first two positions but replaces the third with cytidine. Phenylalanine decoding of UUU and UUC also differed in the third-position pairing geometry. One possibility is that an Et1Ψ residue at the third codon position, the cumulative presence of three adjacent Et1Ψ residues, or both is less compatible with efficient tRNA accommodation. A larger N1-ethyl substituent may alter local base stacking, codon-anticodon geometry, or decoding kinetics; however, these possibilities were not directly tested. Sequence- and position-dependent effects on decoding have also been reported for Ψ- and m1Ψ-containing codons.[16] More broadly, studies of non-standard codon nucleotides, pseudouridylated coding sequences, codon bias, and codon optimality show that codon context can influence translation and mRNA stability.[19–22] These observations support the broader concept that modified-nucleoside performance depends on sequence context but do not establish the mechanism responsible for the Et1Ψ-UUU interaction. Therefore, our mechanistic interpretation should be considered a working hypothesis. We did not directly measure ribosome dwell time, tRNA selection or accommodation kinetics, codon-specific pausing, or the structure of an Et1Ψ-containing codon within the decoding center. Ribosome profiling, reconstituted translation assays, and structural studies are required to determine whether the

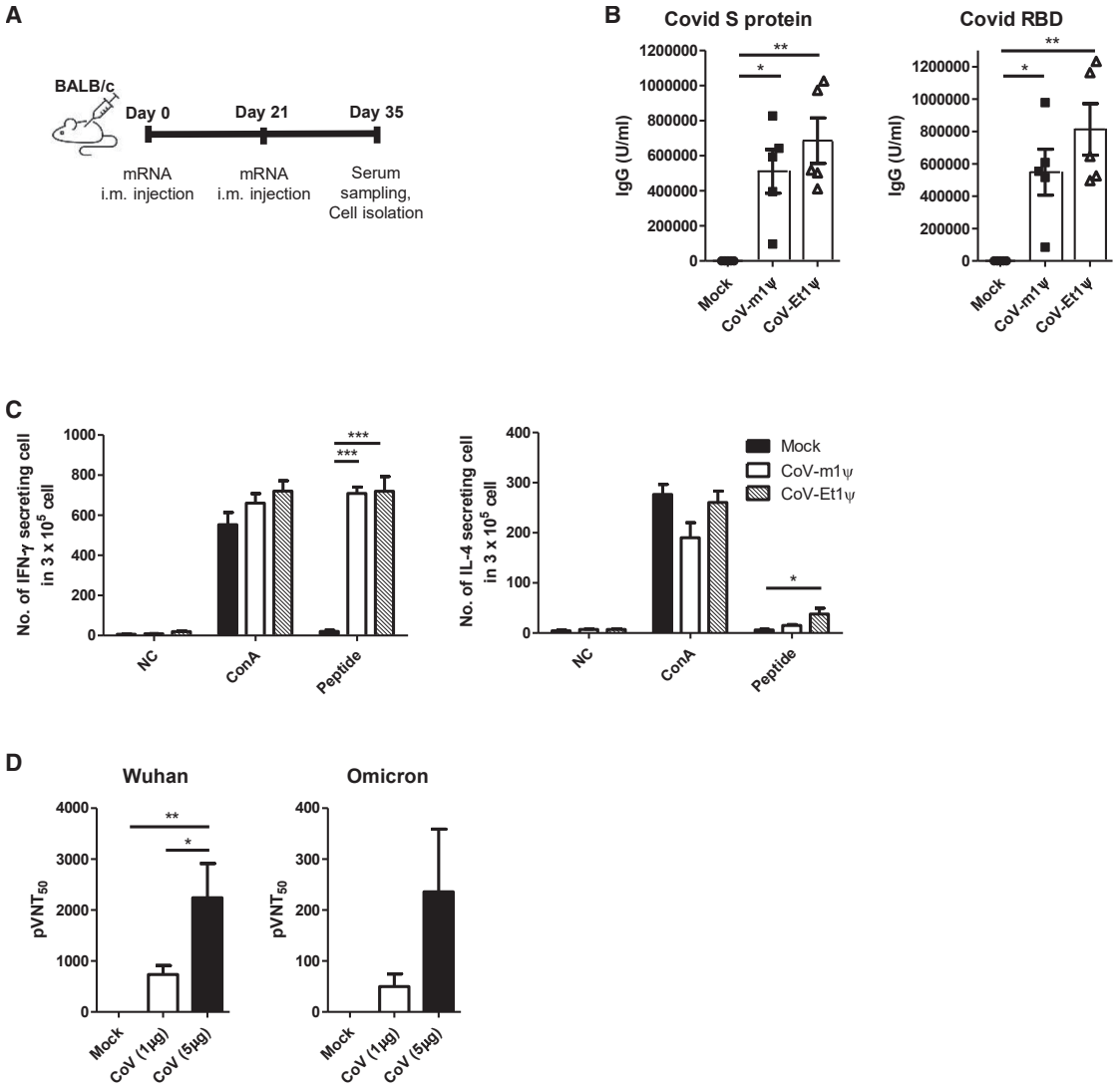


Figure 4. Adaptive immune responses after SARS-CoV-2 spike mRNA-LNP vaccination

(A) Immunization and sampling schedule. BALB/c mice received spike mRNA-LNP on days 0 and 21, and serum and splenocytes were collected on day 35. (B) S1- and RBD-specific serum IgG measured by ELISA ($n = 5$ mice per group). (C) IFN-γ- and IL-4-secreting splenocytes measured by ELISPOT after stimulation with spike peptide pools ($n = 5$ mice per group). Medium and concanavalin A (ConA) served as negative and positive controls, respectively. (D) Neutralizing antibody titers against ancestral Wuhan and Omicron pseudoviruses ($n = 9$ mice per group). In (B) and (C), each symbol represents one mouse (one biological replicate), and symbol shapes correspond to the treatment groups shown in the graphs. Data are presented as mean ± SD. Statistical significance was assessed by one-way ANOVA with Tukey's multiple-comparison test; $^{*}p < 0.05$, $^{**}p < 0.01$, $^{***}p < 0.001$.

observed phenotype reflects steric interference, altered wobble pairing, changes in local RNA structure, or another step in translation. Although we did not observe changes in electrophoretic mobility or vaccine immunogenicity suggestive of major translation errors, translational fidelity was not directly assessed using mass spectrometry.

The sequence modification used was deliberately limited in scope. Every phenylalanine-encoding UUU codon in the open reading frame was replaced with UUC without additional synonymous recoding or alteration of the encoded amino acid sequence. Conventional mRNA optimization strategies typically consider parameters, such as codon usage, GC content, and RNA secondary structure but may not explicitly require the complete exclusion of a specific codon.[23] For example, recent mRNA design algorithms jointly optimize codon usage and RNA structural stability, whereas other therapeutic mRNA design frameworks implement uridine depletion as a separate, explicit sequence constraint.[24] Thus, depending on the optimization strategy and its objectives, a codon-optimized sequence may retain UUU codons unless their exclusion is specifically

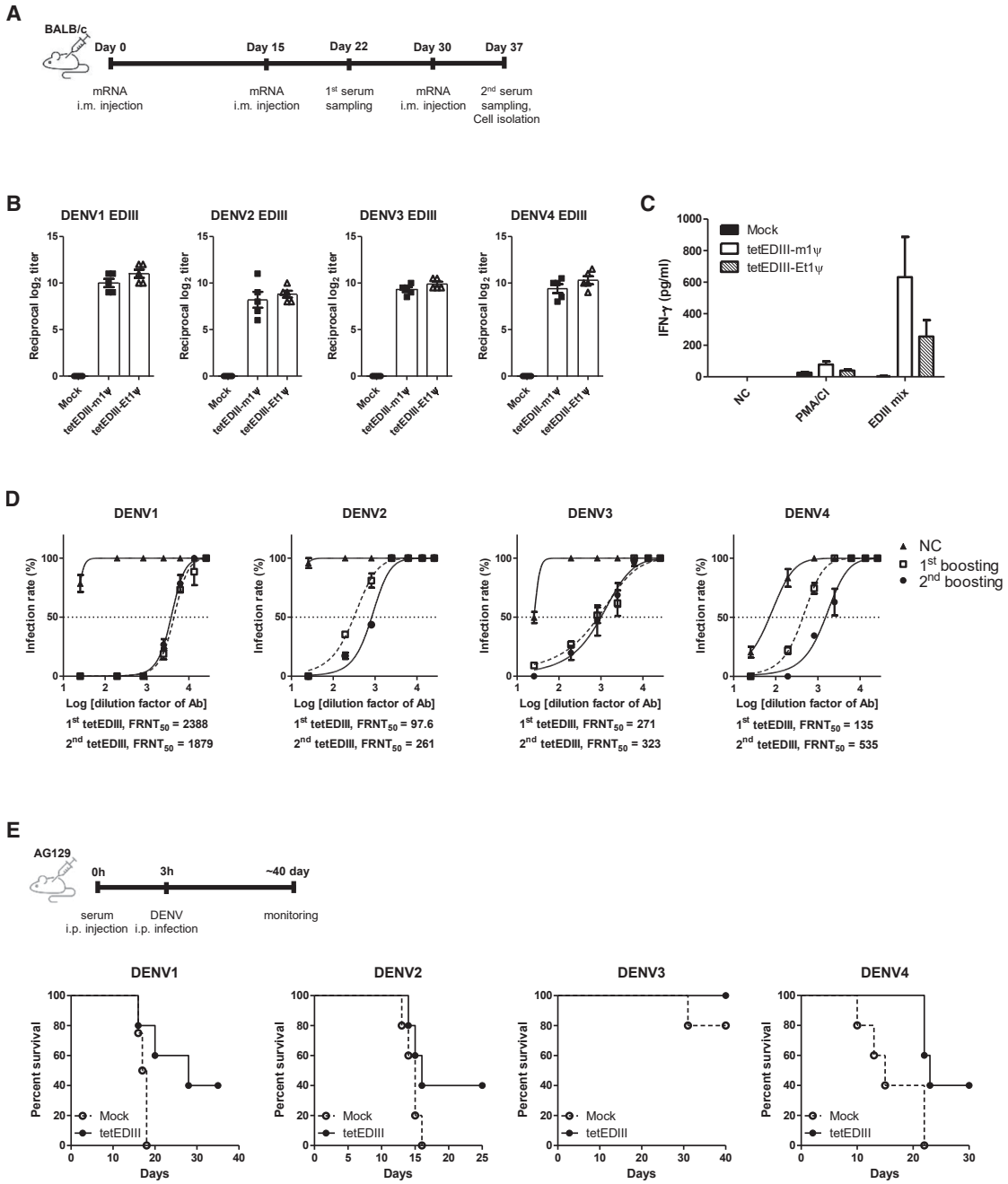


Figure 5. Immune responses and passive protection after dengue tetEDIII mRNA-LNP vaccination

(A) Dengue immunization, serum collection, and challenge schedule. BALB/c mice were immunized with DENV tetEDIII mRNA-LNP on days 0, 15, and 30 (5 μg; *n* = 5 mice per group). (B) Endpoint IgG titers against DENV1-4 EDIII measured by ELISA. Each symbol represents one mouse (one biological replicate), and symbol shapes correspond to the treatment groups shown in the graph. (C) IFN-γ production after splenocyte restimulation, measured by cytometric bead array (CBA). PMA/CI denotes phorbol 12-myristate 13-acetate plus calcium ionophore (ionomycin). (D) Focus reduction neutralization test (FRNT) against DENV1-4 using serum samples collected after the first and second boosts. Serum samples from five mice per vaccination group were pooled at each time point and then analyzed in technical triplicate. NC denotes negative-control serum; distinct symbols identify NC, first-boost, and second-boost samples. (E) Passive serum transfer and DENV challenge in AG129 mice. Mice received immune serum intraperitoneally, were challenged 3 h later, and were monitored for survival for up to 40 days (*n* = 5 mice per challenge group).

imposed. The prevalence of UUU-rich coding sequences among therapeutic mRNAs has not been systematically characterized and may vary with the encoded protein and sequence design strategy. For Et1Ψ-containing mRNAs, UUU exclusion could therefore be considered an additional sequence design constraint. UUU can be synonymously replaced with UUC without changing the encoded amino acid. Thus, this constraint could be incorporated into existing sequence design workflows. However, the effects of recoding on local RNA structure, stability, and expression should be evaluated for each construct.

Et1Ψ consistently showed a reduced innate immune activation profile. In THP-1 reporter cells, Et1Ψ induced less IRF-dependent activity than unmodified uridine and m1Ψ. In mice, Et1Ψ reduced early IFN-α and IFN-γ responses and lowered several inflammatory mediators; in the spike mRNA experiment, the levels of CXCL10 and MCP-1 were also lower than those after m1Ψ treatment. Excessive activation of RNA-sensing pathways can restrict mRNA translation and promote RNA turnover,[25,26] suggesting that moderate innate signaling may be advantageous in settings where early systemic inflammation is undesirable. Nevertheless, the present cytokine measurements were limited to selected analytes and early time points and did not establish broader clinical safety or superiority. Reduced early innate signaling did not compromise adaptive immune responses in the tested vaccine models. Codon-adjusted Et1Ψ mRNA-LNP elicited SARS-CoV-2 antigen-specific IgG, Th1-skewed cellular responses, and neutralizing activity comparable to m1Ψ, consistent with previous observations that nucleoside-modified mRNA can retain strong adaptive immunogenicity despite reduced innate sensing.[6,18] Dengue vaccine development is particularly sensitive to serotype balance and ADE.[27,28] Epidemiologic evidence further supports an association between antibody response magnitude and the risk of severe dengue disease.[29] In the tetravalent dengue model, Et1Ψ induced antibody and cellular responses against all four serotypes, and booster immunization broadened the neutralization profile. Passive-transfer protection was serotype dependent, and the limited lethality of the DENV3 control group reduced the dynamic range of the challenge. These findings support the feasibility of Et1Ψ in more than one antigen context while emphasizing that immune balance and protective efficacy remain dependent on antigen design and the experimental model.

In conclusion, Et1Ψ is a candidate alternative nucleoside modification with a defined sequence design requirement. UUU codons can limit Et1Ψ-driven translation, but targeted UUU-to-UUC recoding restored expression while preserving vaccine immunogenicity and a reduced early innate immune profile under the conditions tested. These results identify codon-modification compatibility as a practical design principle and support further mechanistic and translational evaluation of Et1Ψ-based mRNA.

MATERIALS AND METHODS

Experimental materials and animals

Unless otherwise specified, the chemicals and laboratory wares used were purchased from Sigma Chemical Co. (St. Louis, MO, USA) and SPL Life Sciences (Pocheon, Korea), respectively. Specific pathogen-free female BALB/c mice (8–12 weeks old) were purchased from Koatech (Pyeongtaek, Korea) and acclimated for one week. All procedures were approved by the Institutional Animal Care and Use Committee (IACUC) of mCureX Therapeutics (approval no. MCX-IACUC-AP-202303) and conducted in accordance with the relevant ethical guidelines. AG129 mice, which are deficient in type I and II IFN receptors, were purchased from Marshall BioResources (Hull, East Yorkshire, UK) and maintained under standard specific pathogen-free conditions with *ad libitum* access to food and water. A group of 3–5 mice was used in each experiment, and procedures involving animals were approved by the Institutional Animal Care and Use Committee of Jeonbuk National University (approval number: JBNU-NON2024-038) and followed the guidelines recommended by the committee.

Cell culture

HEK293 and HeLa cells were cultured in Dulbecco's Modified Eagle Medium (DMEM; Gibco) supplemented with 10% fetal bovine serum (FBS) and 1% penicillin-streptomycin at 37°C in 5% CO_2. Vero E6 cells (American Type Culture Collection [ATCC], Manassas, VA, USA) were used for viral neutralization assays and DENV propagation. The cells were cultured in DMEM (Welgene, Gyeongsan, Korea) supplemented with 5% FBS (Gibco, Thermo Fisher Scientific, Grand Island, NY, USA).

In vitro transcription and codon optimization

The mRNA constructs encoding the SARS-CoV-2 spike (S) and DENV tetEDIII were synthesized by T7 RNA polymerase-mediated *in vitro* transcription (IVT). Co-transcriptional capping was performed using CleanCap AG (TriLink Biotechnologies, San Diego, CA, USA) to generate a cap 1 structure. During IVT, uridine was fully replaced with either m1Ψ or Et1Ψ. For the UUU-depleted variants, every phenylalanine-encoding UUU codon within the open reading frame was replaced with UUC to preserve the amino acid sequence. No broader codon optimization algorithm or additional synonymous recoding was used for this comparison. The transcribed mRNAs were purified using the RNeasy Maxi Kit (QIAGEN, Hilden, Germany) to remove template DNA and reaction impurities.

Preparation and characterization of mRNA-loading LNPs

mRNA-LNPs were formulated using a lipid mixture of SM-102, cholesterol, DSPC, and PEG2000-DMG at a fixed molar ratio of 50:38.5:10:1.5, based on a previously reported formulation.[30] The lipids were dissolved in ethanol to a final concentration of 8.80 mg/mL, and the mRNA was diluted in 6.25 mM sodium acetate buffer (pH 5.0). The lipid and mRNA solutions were mixed at a 3:1 aqueous-to-organic flow rate ratio using a microfluidic mixer (Precision NanoSystems, Vancouver, BC, Canada). To remove residual ethanol and facilitate buffer exchange, the LNP dispersion was purified and concentrated via centrifugal filtration using Amicon Ultra-15 centrifugal filter units (100 kDa MWCO; Millipore Sigma, Burlington, MA, USA).[31] The formulation was exchanged into the final storage buffer, which consists of 20 mM Tris, 87 mg/mL (8.7%)

sucrose, and 10.7 mM sodium acetate (pH 7.5). The final mRNA concentration was adjusted to 0.2 mg/mL. LNP size (Z-average) and polydispersity index were measured by dynamic light scattering using a Zetasizer (Malvern Panalytical, Malvern, UK), and mRNA encapsulation efficiency was determined using a Ribogreen fluorometric assay.

In vitro transfection and expression analysis

Cells (HEK293 or HeLa) were seeded at 2×10^5 cells/well in 24-well plates and incubated overnight prior to transfection. mRNA constructs (firefly luciferase [FLuc] with varied UUU frequencies, DENV tetEDIII, or SARS-CoV-2 spike) were transfected at 500 ng/well using Lipofectamine MessengerMAX (Thermo Fisher Scientific) in accordance with the manufacturer's instructions. All transfections were performed in triplicate. At 24 h post-transfection, FLuc activity was quantified as RLU using the Luciferase Assay System (Promega Corporation, Madison, WI, USA). The expression of DENV tetEDIII and SARS-CoV-2 spike was confirmed via western blot using a DENV-specific antibody (D1-11) (Santa Cruz Biotechnology, Dallas, TX, USA) and a CoV spike protein-specific antibody (40591-MM42) (Sino Biological Inc., Beijing, China) to verify molecular weight and protein integrity.

In vitro translation and IRF activity assay in THP-1Dual™ cells

THP1-Dual cells (InvivoGen, San Diego, CA, USA) were maintained in RPMI 1640 supplemented with 10% heat-inactivated FBS, 2 mM L-glutamine, 25 mM HEPES, and Normocin. Cells at passage <20 were differentiated with 20–50 ng/mL PMA for 3 h, followed by a 72 h recovery in fresh medium. To modulate type I IFN signaling, the cells were pretreated with IFNAR1-targeting siRNA or neutralizing anti-IFNAR1 antibody before transfection. Differentiated cells were seeded at 1×10^5 cells/well in 96-well plates. Transfection was performed with 2 μg/mL FLuc or SARS-CoV-2 spike mRNA (U, m1Ψ, or Et1Ψ) using Lipofectamine MessengerMAX. All mRNA samples were prepared in endotoxin-free water to prevent unintended TLR4 activation. IRF pathway activation was assessed by measuring the luciferase activity of the secreted Lucia. At 24 h post-transfection, 20 μL of the supernatant was mixed with 50 μL of QUANTI-Luc (InvivoGen). Bioluminescence was measured using a luminometer with a 0.1 s integration time. Intracellular FLuc activity was quantified in cell lysates using the Luciferase Assay System (Promega). All assays were performed in three independent biological experiments ($n = 3$).

In vivo bioluminescence imaging

To assess *in vivo* translation efficiency of mRNA variants, female BALB/c mice (8–12 weeks old) received a single intravenous (IV) injection of 10 μg of FLuc mRNA packaged with the TransIT-mRNA Transfection Kit (Mirus Bio LLC, Madison, WI, USA). The mRNA was combined with TransIT-mRNA reagent and mRNA Boost at a weight ratio of 1:1.1:0.7 (mRNA:reagent:boost) in DMEM. At 6 h after injection, D-luciferin (150 mg/kg) was administered intraperitoneally. Mice were anesthetized with isoflurane, and bioluminescence was captured using the IVIS Spectrum Imaging System (PerkinElmer). Total flux (photons/sec) was measured with Living Image software to compare the expression levels among unmodified uridine, m1Ψ, and Et1Ψ constructs.

Serum cytokine profiling

A multiplex cytokine assay was conducted to assess the acute systemic inflammatory response and innate immune activation induced by mRNA-LNPs. Female BALB/c mice (12-weeks old) received a single IV injection of 10 μg of mRNA-LNPs ($n = 4$ per group). Poly(I:C) (100 μg per mouse) was administered as a positive control for TLR3-mediated immune activation. At 6 h after injection, blood was collected via cardiac puncture, and serum was isolated by centrifugation at 2,000 × *g* for 15 min at 4°C.

Systemic levels of key pro-inflammatory cytokines and chemokines, including IFN-α, IFN-γ, IL-6, MIP-1α (CCL3), MIP-1β (CCL4), CXCL10 (IP-10), and MCP-1 (CCL2), were measured using a Luminex 200 system (Luminex Corp, Austin, TX, USA). The assay was performed using a Bio-Plex Pro Mouse Cytokine Panel (Bio-Rad Laboratories, Hercules, CA, USA) or a custom ProcartaPlex Mouse Panel (Thermo Fisher Scientific) in accordance with the manufacturer's instructions. Cytokine concentrations were calculated from standard curves generated with recombinant protein standards provided with the kit, and data analysis was performed using Bio-Plex Manager software.

Immunization and sampling

Mice were intramuscularly injected with 1 and 5 μg of SARS-CoV-2 spike mRNA-LNPs synthesized with unmodified U, m1Ψ, or Et1Ψ. Prime immunization was administered on day 0, followed by a booster on day 21.[32] For ELISA and ELISPOT, mice ($n = 5$ per group) were euthanized on day 35 for serum and spleen collection. For pseudovirus neutralization, a separate cohort ($n = 9$ per group) provided serum samples on day 35. For DENV vaccination, female BALB/c mice (5–6 weeks old) were immunized intramuscularly with the mRNA-LNP formulation at the indicated dose (5 μg per mouse). Primary immunization was administered on day 0, followed by a first booster on day 15, and a second booster on day 30. Serum samples were collected on day 22 to assess the humoral immune responses. A terminal serum sample was collected on day 37, and spleens were harvested for cellular immune analyses. Serum samples were isolated by centrifugation and stored at −80°C until use.

Antibody-binding assay

Serum IgG titers against SARS-CoV-2 S1 and RBD were measured using ELISA kits (Alpha Diagnostic International, San Antonio, TX, USA) in accordance with the manufacturer's instructions. Splenocytes were isolated via mechanical disruption and red blood cell lysis. Splenocytes at 5×10^5 per well were stimulated with SARS-CoV-2 spike peptide pools (2 μg/mL) to assess cellular immunity. DENV-specific immunoglobulin levels in serum were measured using direct ELISA as described previously.[33] In brief, each EDIII protein (1 μg/mL) was diluted in 0.05 M carbonate-bicarbonate coating buffer (pH 9.6), and 100 μL per well was used to coat 96-well plates

(Nunc, Thermo Fisher Scientific, Roskilde, Denmark) overnight at 4°C. The plates were washed with PBST and blocked with 3% skim milk for 1 h at room temperature (RT). After washing, 100 μL of 2-fold serially diluted serum samples was added to each well and incubated for 2 h at RT. The plates were washed again and then incubated with an alkaline phosphatase-conjugated anti-mouse IgG secondary antibody (Sigma-Aldrich) for 1 h at RT. After a final wash, the substrate solution was added, and the absorbance was measured at 405 nm using a microplate reader (BMG Labtech, Ortenberg, Germany).

Tissue sampling and analysis

To evaluate cellular immune responses, the mice were sacrificed by cervical dislocation, and their spleens were aseptically removed. The spleens were mechanically dissociated through a 40 μm cell strainer to obtain single-cell suspensions, which were then washed with cold PBS. The cell pellets were resuspended in 4 mL of 40% Percoll (Amersham Pharmacia Biotech, Piscataway, NJ, USA). The cell suspension was carefully layered onto a 75% Percoll gradient and then centrifuged at 800 × *g* for 20 min at RT without a break. The mononuclear cells were collected from the interface between the 40% and 75% Percoll layers and washed with PBS. Residual red blood cells were lysed using RBC lysis buffer in accordance with the manufacturer's instructions. The resulting splenocytes were analyzed for cytokines using an ELISPOT kit (Mabtech AB, Nacka Strand, Sweden) or a cytometric bead array (BD Biosciences, San Jose, CA, USA).

Neutralization assay against SARS-CoV-2 and DENV

Neutralizing activity was assessed using luciferase-expressing pseudoviruses such as U0401 for the prototype and U0416 for Omicron (Abnova Corporation, Taipei, Taiwan). Heat-inactivated serum samples were serially diluted and incubated with pseudoviruses for 30 min at RT. The mixture was added to HEK293T-hACE2 cells (GenScript Biotech Corporation, Piscataway, NJ, USA) seeded at 1×10^5 cells/well. After 48 h, luciferase activity was measured (Promega), and the half-maximal inhibitory dilution (pVNT50) was determined using nonlinear regression analysis. For FRNTs, the serum samples were mixed with DENV and incubated for 1 h at 37°C. Then, the mixture was applied to Vero E6 cells (approximately 100–150 spots per well) that had been plated in a 96-well plate 1 day prior and then incubated for 1 h at 37°C. Afterward, the overlay medium was added, and the plate was incubated for 3 days. Finally, the spots were developed to count FFUs, and the FRNT was calculated relative to the untreated samples and expressed as a percentage.

DENV challenge infection in AG129 mice

For passive protection experiments, 30 μL of immune serum diluted in PBS to a total volume of 100 μL was administered intraperitoneally to age- and weight-matched AG129 mice. At 3 h after serum transfer, the mice were challenged i.p. with the indicated doses of DENV serotypes: DENV1 (3×10^6 FFU), DENV2 (1×10^6 FFU), DENV3 (1×10^7 FFU), or DENV4 (5×10^6 FFU). The mice were monitored daily for survival and clinical signs of the disease for up to 40 days post-infection. Mortality was recorded, and survival curves were generated using the Kaplan-Meier method.

Statistical analysis

Statistical analyses were performed using Prism version 6 or 9 (GraphPad Software, La Jolla, CA, USA). Data are presented as mean ± SD or mean ± SEM, as specified in each figure legend. For *in vitro* assays, n denotes independent biological experiments, and technical replicate wells were averaged within each experiment. For animal studies, n denotes individual animals, unless otherwise stated. For the dengue FRNT assay, serum samples from five mice per vaccination group were pooled at each time point, and the pooled samples were analyzed in technical triplicate. The technical replicates were not treated as independent biological replicates. Multiple-group comparisons were performed using one-way analysis of variance (ANOVA) with Tukey's multiple comparison test. Statistical significance was defined as $p < 0.05$. The animals were randomly assigned to the experimental groups, and the investigators were not blinded during the outcome assessment.

DATA AND CODE AVAILABILITY

Data are available from the corresponding author upon reasonable request.

ACKNOWLEDGMENTS

This work was supported by the Vaccine Self-Sufficiency Technology Development Program through the Korea Health Industry Development Institute, funded by the Ministry of Health and Welfare, Republic of Korea (RS-2024-00335889), by a grant of Korean ARPA-H Project through the Korea Health Industry Development Institute (KHIDI), funded by the Ministry of Health & Welfare, Republic of Korea (RS-2024-00507559), and by the Advanced Technology Center Plus (ATC+) Program through the Korea Evaluation Institute of Industrial Technology (KEIT), funded by the Ministry of Trade, Industry and Energy, Republic of Korea (RS-2023-KT222864). The funders had no role in the study design, data collection and analysis, decision to publish, or manuscript preparation.

AUTHOR CONTRIBUTIONS

K.K., G.L, J.P., Y.-S.J., and S.L. conceived the study. J.P., G.L., H.L., and J.L. developed the methodology. J.K., K.K., E.K., Y.-S.J., S.L., and J.Y. performed the experiments. G.L. and J.P. conducted the formal analyses. J.P., Y.-S.J., S.L., and J.Y. curated the data. Y.-S.J. and S.L. acquired funding. J.P. and G.L. drafted the original manuscript. Y.-S.J. and J.Y. reviewed and edited the manuscript.

DECLARATION OF INTERESTS

G.L. and S.L. are employees of mCureX Therapeutics. K.K., E.K., and J.L. were employees of mCureX Therapeutics at the time this work was performed and are currently employees of Daehan Nupharm Co., Ltd.

DECLARATION OF GENERATIVE AI AND AI-ASSISTED TECHNOLOGIES IN THE WRITING PROCESS

During the preparation of this work the authors used artificial intelligence tools, such as Grammarly Insights and ChatGPT, to refine English language by improving fluency and correcting grammatical errors. After using these tools, the authors reviewed and edited the content as needed and take full responsibility for the content of the publication.

REFERENCES

1. Wolff, J.A., Malone, R.W., Williams, P., Chong, W., Acsadi, G., Jani, A., and Felgner, P.L. (1990). Direct gene transfer into mouse muscle in vivo. Science *247*, 1465–1468. https://doi.org/10.1126/science.1690918.

2. Sahin, U., Karikó, K., and Türeci, Ö. (2014). mRNA-based therapeutics–developing a new class of drugs. Nat. Rev. Drug Discov. *13*, 759–780. https://doi.org/10.1038/nrd4278.

3. Gote, V., Bolla, P.K., Kommineni, N., Butreddy, A., Nukala, P.K., Palakurthi, S.S., and Khan, W. (2023). A Comprehensive Review of mRNA Vaccines. Int. J. Mol. Sci. *24*, 2700. https://doi.org/10.3390/ijms24032700.

4. Verbeke, R., Hogan, M.J., Loré, K., and Pardi, N. (2022). Innate immune mechanisms of mRNA vaccines. Immunity *55*, 1993–2005. https://doi.org/10.1016/j.immuni.2022.10.014.

5. Leong, K.Y., Tham, S.K., and Poh, C.L. (2025). Revolutionizing immunization: a comprehensive review of mRNA vaccine technology and applications. Virol. J. *22*, 71. https://doi.org/10.1186/s12985-025-02645-6.

6. Pardi, N., Hogan, M.J., Porter, F.W., and Weissman, D. (2018). mRNA vaccines - a new era in vaccinology. Nat. Rev. Drug Discov. *17*, 261–279. https://doi.org/10.1038/nrd.2017.243.

7. Baden, L.R., El Sahly, H.M., Essink, B., Kotloff, K., Frey, S., Novak, R., Diemert, D., Spector, S.A., Rouphael, N., Creech, C.B., et al. (2021). Efficacy and Safety of the mRNA-1273 SARS-CoV-2 Vaccine. N. Engl. J. Med. *384*, 403–416. https://doi.org/10.1056/nejmoa2035389.

8. Hou, X., Zaks, T., Langer, R., and Dong, Y. (2021). Lipid nanoparticles for mRNA delivery. Nat. Rev. Mater. *6*, 1078–1094. https://doi.org/10.1038/s41578-021-00358-0.

9. Dolgin, E. (2021). The tangled history of mRNA vaccines. Nature *597*, 318–324. https://doi.org/10.1038/d41586-021-02483-w.

10. Borchardt, E.K., Martinez, N.M., and Gilbert, W.V. (2020). Regulation and Function of RNA Pseudouridylation in Human Cells. Annu. Rev. Genet. *54*, 309–336. https://doi.org/10.1146/annurev-genet-112618-043830.

11. Bérouti, M., Wagner, M., Greulich, W., Piseddu, I., Gärtig, J., Hansbauer, L., Müller-Hermes, C., Heiss, M., Pichler, A., Tölke, A.J., et al. (2025). Pseudouridine RNA avoids immune detection through impaired endolysosomal processing and TLR engagement. Cell *188*, 4880–4895.e15. https://doi.org/10.1016/j.cell.2025.05.032.

12. Li, C., Lee, A., Grigoryan, L., Arunachalam, P.S., Scott, M.K.D., Trisal, M., Wimmers, F., Sanyal, M., Weidenbacher, P.A., Feng, Y., et al. (2022). Mechanisms of innate and adaptive immunity to the Pfizer-BioNTech BNT162b2 vaccine. Nat. Immunol. *23*, 543–555. https://doi.org/10.1038/s41590-022-01163-9.

13. Andries, O., Mc Cafferty, S., De Smedt, S.C., Weiss, R., Sanders, N.N., and Kitada, T. (2015). N(1)-methylpseudouridine-incorporated mRNA outperforms pseudouridine-incorporated mRNA by providing enhanced protein expression and reduced immunogenicity in mammalian cell lines and mice. J. Control. Release *217*, 337–344. https://doi.org/10.1016/j.jconrel.2015.08.051.

14. Komar, A.A. (2016). The Yin and Yang of codon usage. Hum. Mol. Genet. *25*, R77–R85. https://doi.org/10.1093/hmg/ddw207.

15. Bazzini, A.A., Del Viso, F., Moreno-Mateos, M.A., Johnstone, T.G., Vejnar, C.E., Qin, Y., Yao, J., Khokha, M.K., and Giraldez, A.J. (2016). Codon identity regulates mRNA stability and translation efficiency during the maternal-to-zygotic transition. EMBO J. *35*, 2087–2103. https://doi.org/10.15252/embj.201694699.

16. Monroe, J., Eyler, D.E., Mitchell, L., Deb, I., Bojanowski, A., Srinivas, P., Dunham, C.M., Roy, B., Frank, A.T., and Koutmou, K.S. (2024). N1-Methylpseudouridine and pseudouridine modifications modulate mRNA decoding during translation. Nat. Commun. *15*, 8119. https://doi.org/10.1038/s41467-024-51301-0.

17. Kuzmin, I.V., Soto Acosta, R., Pruitt, L., Wasdin, P.T., Kedarinath, K., Hernandez, K.R., Gonzales, K.A., Hill, K., Weidner, N.G., Mire, C., et al. (2024). Comparison of uridine and N1-methylpseudouridine mRNA platforms in development of an Andes virus vaccine. Nat. Commun. *15*, 6421. https://doi.org/10.1038/s41467-024-50774-3.

18. Karikó, K., Muramatsu, H., Welsh, F.A., Ludwig, J., Kato, H., Akira, S., and Weissman, D. (2008). Incorporation of pseudouridine into mRNA yields superior nonimmunogenic vector with increased translational capacity and biological stability. Mol. Ther. *16*, 1833–1840. https://doi.org/10.1038/mt.2008.200.

19. Hoernes, T.P., Faserl, K., Juen, M.A., Kremser, J., Gasser, C., Fuchs, E., Shi, X., Siewert, A., Lindner, H., Kreutz, C., et al. (2018). Translation of non-standard codon nucleotides reveals minimal requirements for codon-anticodon interactions. Nat. Commun. *9*, 4865. https://doi.org/10.1038/s41467-018-07321-8.

20. Eyler, D.E., Franco, M.K., Batool, Z., Wu, M.Z., Dubuke, M.L., Dobosz-Bartoszek, M., Jones, J.D., Polikanov, Y.S., Roy, B., and Koutmou, K.S. (2019). Pseudouridinylation of mRNA coding sequences alters translation. Proc. Natl. Acad. Sci. USA *116*, 23068–23074. https://doi.org/10.1073/pnas.1821754116.

21. Plotkin, J.B., and Kudla, G. (2011). Synonymous but not the same: the causes and consequences of codon bias. Nat. Rev. Genet. *12*, 32–42. https://doi.org/10.1038/nrg2899.

22. Presnyak, V., Alhusaini, N., Chen, Y.H., Martin, S., Morris, N., Kline, N., Olson, S., Weinberg, D., Baker, K.E., Graveley, B.R., and Coller, J. (2015). Codon optimality is a major determinant of mRNA stability. Cell *160*, 1111–1124. https://doi.org/10.1016/j.cell.2015.02.029.

23. Zhang, H., Zhang, L., Lin, A., Xu, C., Li, Z., Liu, K., Liu, B., Ma, X., Zhao, F., Jiang, H., et al. (2023). Algorithm for optimized mRNA design improves stability and immunogenicity. Nature *621*, 396–403. https://doi.org/10.1038/s41586-023-06127-z.

24. Vostrosablin, N., Lim, S., Gopal, P., Brazdilova, K., Parajuli, S., Wei, X., Gromek, A., Prihoda, D., Spale, M., Muzdalo, A., et al. (2024). mRNAid, an open-source platform for therapeutic mRNA design and optimization strategies. NAR Genom. Bioinform. *6*, lqae028. https://doi.org/10.1093/nargab/lqae028.

25. Loo, Y.M., and Gale, M., Jr. (2011). Immune signaling by RIG-I-like receptors. Immunity *34*, 680–692. https://doi.org/10.1016/j.immuni.2011.05.003.

26. Ivashkiv, L.B., and Donlin, L.T. (2014). Regulation of type I interferon responses. Nat. Rev. Immunol. *14*, 36–49. https://doi.org/10.1038/nri3581.

27. Halstead, S.B. (2014). Dengue Antibody-Dependent Enhancement: Knowns and Unknowns. Microbiol. Spectr. *2*. https://doi.org/10.1128/microbiolspec.AID-0022-2014.

28. Sridhar, S., Luedtke, A., Langevin, E., Zhu, M., Bonaparte, M., Machabert, T., Savarino, S., Zambrano, B., Moureau, A., Khromava, A., et al. (2018). Effect of Dengue Serostatus on Dengue Vaccine Safety and Efficacy. N. Engl. J. Med. *379*, 327–340. https://doi.org/10.1056/NEJMoa1800820.

29. Katzelnick, L.C., Gresh, L., Halloran, M.E., Mercado, J.C., Kuan, G., Gordon, A., Balmaseda, A., and Harris, E. (2017). Antibody-dependent enhancement of severe dengue disease in humans. Science *358*, 929–932. https://doi.org/10.1126/science.aan6836.

30. ModernaTX, Inc (2020). A phase 3, randomized, stratified, observer-blind, placebo-controlled study to evaluate the efficacy, safety, and immunogenicity of mRNA-1273 SARS-CoV-2 vaccine in adults aged 18 years and older. https://clinicaltrials.gov/study/NCT04470427.

31. Schober, G.B., Story, S., and Arya, D.P. (2024). A careful look at lipid nanoparticle characterization: analysis of benchmark formulations for encapsulation of RNA cargo size gradient. Sci. Rep. *14*, 2403. https://doi.org/10.1038/s41598-024-52685-1.

32. Hassett, K.J., Benenato, K.E., Jacquinet, E., Lee, A., Woods, A., Yuzhakov, O., Himansu, S., Deterling, J., Geilich, B.M., Ketova, T., et al. (2019). Optimization of Lipid Nanoparticles for Intramuscular Administration of mRNA Vaccines. Mol. Ther. Nucleic Acids *15*, 1–11. https://doi.org/10.1016/j.omtn.2019.01.013.

33. Park, J., Lee, H.Y., Khai, L.T., Thuy, N.T.T., Mai, L.Q., and Jang, Y.S. (2020). Addition of Partial Envelope Domain II into Envelope Domain III of Dengue Virus Antigen Potentiates the Induction of Virus-Neutralizing Antibodies and Induces Protective Immunity. Vaccines (Basel) *8*, 88. https://doi.org/10.3390/vaccines8010088.